2017

NONLINEAR DIELECTRIC BEHAVIOR OF FIELD-INDUCED ANTIFERROELECTRIC/PARAELECTRIC-TO-FERROELECTRIC PHASE TRANSITION FOR HIGH ENERGY DENSITY CAPACITOR APPLICATION

Mingyang Li
Michigan Technological University, mli7@mtu.edu

NONLINEAR DIELECTRIC BEHAVIOR OF FIELD-INDUCED ANTIFERROELECTRIC/PARAELECTRIC-TO-FERROELECTRIC PHASE TRANSITION FOR HIGH ENERGY DENSITY CAPACITOR APPLICATION

By

Mingyang Li

A THESIS

Submitted in partial fulfillment of the requirements for the degree of

MASTER OF SCIENCE

In Materials Science and Engineering

MICHIGAN TECHNOLOGICAL UNIVERSITY

2017

This thesis has been approved in partial fulfillment of the requirements for the Degree of MASTER OF SCIENCE in Materials Science and Engineering.

Department of Materials Science & Engineering

Thesis Advisor: *Yu Wang*

Committee Member: *Stephen L. Kampe*

Committee Member: *Stephen A. Hackney*

Department Chair: *Stephen L. Kampe*

Table of Contents

Abstract

Electric field-induced antiferroelectric(AFE)/paraelectric(PE)-to-ferroelectric(FE) phase transitions are investigated for the associated nonlinear dielectric behavior, which could offer high dielectric capacity. The phenomenon in monolithic materials has been computed for Kittel antiferroelectric and $BaTiO_3$ model systems using the Landau-Ginzburg-Devonshire theory. The general switching curves give values of the polarization as a function of external electric field. A similar computation is performed for particle-filled polymer-matrix composites where an internal depolarization field is considered. The polarization-electric field response changes with different depolarization factors, which demonstrate the shape and alignment of the dielectric particles embedded in polymer-matrix are key factors for composite to achieve high dielectric capacity.

1. Introduction

1.1 Nonlinear Dielectric Behavior for High Energy Density Capacitor Application

High energy density capacitors require dielectric materials to have large dielectric constants, and high breakdown strength. In general, most dielectric materials exhibit linear dependence of polarization on electric field. According to the polarization versus electric field response behavior, we can divide all dielectric materials into four types[1]: (1) linear, (2) ferroelectric (FE), (3) relaxor ferroelectric (RFE), and (4) anti-ferroelectric (AFE). The electric energy density stored is described using $U = \int_0^E EdP$, shown as the dark area in Fig. (1), which illustrates the nonlinear dielectric behavior of four different types of dielectric materials.

Linear dielectrics like glassy materials are often characterized by their low dielectric constant and high dielectric breakdown strength[2]. However, materials with low dielectric constant cannot possess high energy density. Ferroelectricity is a property of certain materials that have a spontaneous electric polarization and can be reversed by external electric field. Materials that exhibit ferroelectric material are defined as FE

materials. As shown in Fig. (1b), FE materials have early polarization saturation and possess a large dielectric constant but also lower dielectric breakdown strength, which makes them not perform well at high electric field. Compared to FE materials, relaxor ferroelectrics (RFE) possess much less remnant polarization and coercive electric field while also displaying a slim ferroelectric hysteresis. Thus, RFE are considered to be a better dielectrics than conventional FE materials for capacitor applications. Nevertheless, the study of RFE are restricted for two reasons: (1) these materials are relatively rare[3], and (2) most of these materials are lead-based which are not environmentally friendly. In Fig. (3d), the polarization-electric curve possesses the highest energy storage density. These materials are named anti-ferroelectrics (AFE) since the adjacent dipoles are oriented in opposite directions, which is contrasted to FE materials. AFE materials possess higher energy storage density due to the AFE-to-FE phase transition. At low electric field, AFE materials have no ferroelectric domains which makes them possess low remnant polarization and dielectric loss. The dipoles rotates to the same directions at high electric fields and forms ferroelectric domains. This behavior proves AFE materials are capable of higher density of energy storage. Hence, AFE materials tend to be a suitable choice for high energy density capacitors.

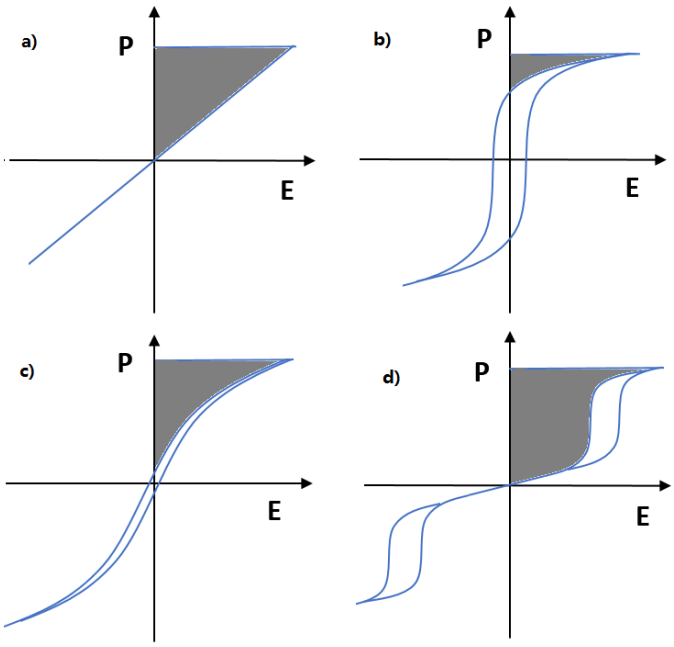

Figure 1 The P-E responses and energy storage characteristics of four classes of dielectric materials.

Dark area represents energy storeds. (a) Linear, (b) FE, (c) relaxor FE, (d) AFE

1.2 Ferroelectric Material and Field-Induced Phase Transition to FE State

In 1921, J.Valasek discovered the phenomenon of ferroelectricity from the dielectric properties of Rochelle salt ($NaKC_4H_4O_6.4H_2O$)[4]. Moreover, the first hysteresis loop of a ferroelectric material is published in the same paper, which reveals the analogy between ferroelectricity and ferromagnetism. Barium titanate ($BaTiO_3$), known as the most famous ferroelectric material, was discovered to be ferroelectric in 1950 by A Von Hippel[5]. FE materials have a wide range of useful properties corresponding to various applications. For instance, high permittivity for capacitors, high piezoelectric effects

for sensors, and high ferroelectric hysteresis for nonvolatile memories. Furthermore, ferroelectrics can be made in different forms, including polymers, single crystals, and thin films according to different requirements.

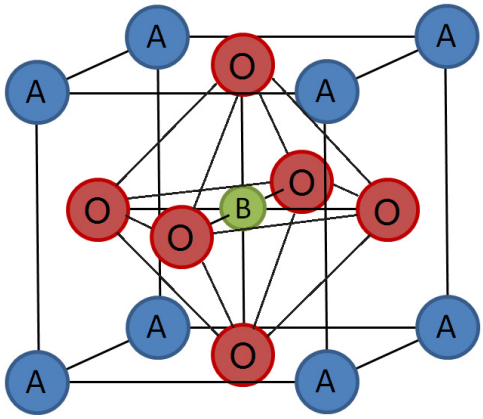

Figure 2 Schematic of cubic perovskite unit cell

Most FE materials have a perovskite structure represented by the chemical formula of ABO_3 where A-site ions are on the corners of the lattice and B-site ions are on the center of the lattice[6, 7]. The simplest cubic perovskite crystal is shown in Fig. (2), where A is an alkali or alkaline earth metal and B belongs to the transition group elements. The transition group element is surrounded by six oxygen atoms giving rise to the BO_6 octahedra[6]. When the atom is eccentrically placed, the charge centers separated and gives rise to a permanent dipole that consists of a pair of electrical charges (positive and negative) [1] . Adjacent dipoles are aligned parallel to each other

and form ferroelectric domains. In FE materials, the direction of spontaneous polarization can be switched by an applied electric field, known as a main difference between pyroelectric and ferroelectric materials.

All FE materials have a transition temperature called Curie temperature (T_c). The crystal does not exhibit ferroelectricity at a temperature greater than Tc, and this non-polar phase is defined as paraelectric phase. The phase encountered below the Curie point that exhibits ferroelectricity is known as FE phase. In this paper, $BaTiO_3$ is selected as the model system to investigate the electric field-induced phase transition since the thermal properties of $BaTiO_3$ has been well developed. All FE crystals will experience a PE-to-FE or FE-to-PE phase transition when temperature goes through the Curie point. For $BaTiO_3$, it undergoes a tetragonal-to-cubic phase transition upon heating above 130 °C, the Curie point of $BaTiO_3$. In cubic perovskite $BaTiO_3$, a paraelectric phase, the titanium atom locates in the centrosymmetric position of the unit cell and spontaneous polarization does not exist. In tetragonal $BaTiO_3$, ferroelectricity occurs due to the displacement of the titanium atom, the creation of a permanent electric dipole. Conversely, a PE-to-FE phase transition occurs while cooling down the $BaTiO_3$ near 130°C. Generally, the temperature of the maximum dielectric constant corresponds to the Curie temperature[8]. However, at a certain temperature range

higher than Curie temperature, the PE-to-FE phase transition can still occur due to an application of external electric field. Furthermore, the removal of the electric field can lead to the polarization returning back to zero. Such nonlinear behavior, as previously illustrated, can offer large capacity.

1.3 Antiferroelectric Materials and Field-Induced Phase Transition to FE State

Besides the electric field-induced PE-to-FE transition in FE materials, AFE-to-FE phase transition induced by external electric field in AFE materials could also exhibit a nonlinear polarization with a polarization jump at higher field.

An anti-ferroelectric material consists of an ordered array of electric dipoles, but with adjacent dipoles oriented in antiparallel directions[9]. Antiferroelectricity is a physical property of certain materials that can appear or disappear depending on various parameters, such as temperature, pressure, external electric field, and growth method. There is a critical temperature that the antiferroelectricity would disappear if the materials reach the point, known as antiferroelectric Curie point[10]. Similar with FE materials, most AFE materials have a perovskite structure represented by the chemical formula of ABO_3. However, in AFE materials adjacent layers of octahedra have dipoles

aligned in antiparallel[11]. Thus, the total macroscopic spontaneous polarization of AFE is zero because the neighboring dipoles cancel each other out.

Lots of researchers put efforts into AFE materials in the past several decades due to its unique antiferroelectricity properties. For industrial applications like energy conversion devices and capacitors with high energy density and high breakdown voltage[12], AFE materials could be a better replacement of FE materials. $PbZrO_3$ (PZO) has been widely investigated as the famous AFE material, the energy storage density is around $50J/cm^3$ [1, 13]. A high energy density of 18.8 J/cm^3 was achieved in Eu-doped PZO (PEZO) thin film capacitors in previous study, which is much higher than capacitors using FE materials[1].

As aforementioned, the adjacent dipoles in AFE crystal oriented in opposite directions when the electric field is absent. However, an external electric field can cause the dipoles vectors closest to the electric field vectors. Once the electric field has increased beyond a critical field E_c, all the dipoles orient in one direction and form domain structure, as well as ferroelectric behavior. Thus, an electric field-induced AFE-to-FE phase transition can takes place in AFE materials. The critical electric field E_c sensitively dependents on the temperature and the purity of the materials. Furthermore,

the AFE-to-FE phase transition brings the volumetric expansion of the crystal and is sensitive to the applied temperature and stress[14, 15]. As shown in Fig. (3), the minimum electric field required to transform from AFE to the FE phase is called the forward critical field E_f; likewise, the reverse critical field is E_a. These phase transitions occur at both positive and negative electric fields, giving rise to the unique double hysteresis. Due to the field-induced AFE-to-FE phase transition, AFE materials have almost no remnant polarizations and possess lower dielectric losses that greatly increase the energy storage efficiency.

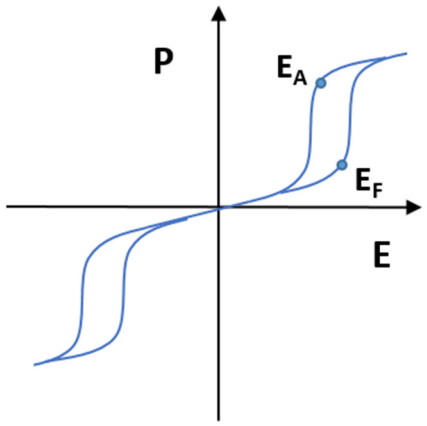

Figure 3 Antiferroelectrics with transition to a ferroelectric phase

2. Theory

2.1 Landau-Ginzburg-Devonshire theory[16]

A phase transition is the transformation of a thermodynamic system from one phase or state of matter to another one by heat transfer. Also, a phase transition occurs when the equilibrium state of a system changes as a function of constraints, which could be pressure, magnetic field, electric field, concentration or any number of other physical quantities[17]. Lev Landau introduces Landau theory, which is a symmetry-based analysis of equilibrium behavior near a phase transition. He proposed that the symmetry of one phase must be higher than that of the other phase because the thermodynamic states of the two phase must be the same at the transition line they shared[18]. Then, Landau characterized the transition in terms of an order parameter, which is the polarization for ferroelectric transition. Furthermore, in the vicinity of a phase transition, we can write down a phenomenological expression for the free energy as a Taylor expansion in the order parameter.

FE materials have attracted much interest since they have been first discovered in 1920[19]. The peculiar behavior of FE materials like spontaneous electric polarization and disappearance of the polarization above a phase transition temperature T_c makes it

a perfect example for the study of phase transitions, electron-phonon interactions and other electrical phenomena[20]. The Landau theory was first applied to ferroelectrics by Devonshire[16] for bulk systems with spatially uniform polarization[18]. Meanwhile, a similar treatment was developed by Ginzburg[21]. The Landau-Ginzburg theory have considered the small spatial variations of the polarization within the phenomenological Landau-Devonshire theory. To specify the thermodynamic state of ferroelectric, four variables should be considered, the temperature, polarization, external electric field, and external elastic stresses. For simplicity, the strain field is ignored and the free energy is expanded in terms of one component polarization. The free energy function for a FE crystal where the origin unpolarized energy is zero is

$$G = \frac{\alpha}{2} P^2 + \frac{\beta}{2} P^4 + \frac{\gamma}{2} P^6 - EP \tag{1}$$

where E is the electric field, α, β and γ are temperature and pressure dependent parameters. The equilibrium conditions correspond to the minimum of G,

$$\frac{\partial G}{\partial P} = 0 \tag{2}$$

The electric field can be calculated directly from the free energy function Eq. (1),

$$E = \frac{\partial G}{\partial P} = \alpha P + \beta P^3 + \gamma P^5 \quad (3)$$

Thus, the nonlinear dependence of the polarization P on the electric field E was introduced.

2.2 Kittel Theory of Antiferroelectric Crystals

In 1951, Charles Kittel[9] defined the antiferroelectric state before AFE materials were experimentally proved to exist. AFE have spontaneous dipoles that are arranged in anti-parallel order, and there is no overall polarization with the absence of electric field. In some certain lattices, the AFE state can be more stable than the FE states. Kittle has also pointed out that the AFE state is not piezoelectric due to the lack of symmetry center. To investigate the dielectric constant near the AFE Curie point, both first-order transition and second-order transition are considered in Kittel's work.

According to the crystal structure of ferroelectrics, Kittel set up a similar model to describe antiferroelectrics. It's a simple tetragonal lattice with highly polarizable ions located at the lattice points and an axial ratio c/a<<1, and the lines of atoms are

considered parallel to the c-axis. Ions in the same line will polarized in a same direction while the neighboring lines of ions will polarized in opposite direction. For simplicity, the lattice is assumed to be decomposed into two identical interpenetrating lattices *a* and b, with corresponding polarizations P_a and P_b. In antiferroelectric state, P_a and P_b have same values but opposite sign. First, a phenomenological expansion for the Helmholtz free energy per unit volume is introduced for AFE, considered as second-order transition,

$$A\left(P_a, P_b, T\right) = A_0 + f(P_a^2 + P_b^2) + gP_aP_b + h\left(P_a^4 + P_b^4\right) \tag{4}$$

where the parameters *f, g*, *h* are functions dependent on temperature values and simply related to polarization and local field constant. The first order derivative of P_a is obtained as

$$\frac{\partial A}{\partial P_a} = E = 2fP_a + gP_b + 4hP_a^3 \tag{5}$$

where E is the electric field. Assuming no electric field is applied, the spontaneous polarization (P_{sa} = - P_{sb}) in AFE state is given by

$$P_{sa}^2 = \frac{(g - 2f)}{4h} \tag{6}$$

Assuming application of a small electric field ΔE and the macroscopic polarization ΔP = $P_a + P_b$, the relationship can be derived as

$$2\Delta E = 2f\Delta P + g\Delta P + 12hP_{sa}^2\Delta P \tag{7}$$

As a result, the susceptibility at Curie point ($g = 2f$) on the AFE side is obtained,

$$\chi_{as} = \frac{\Delta P}{\Delta E} = \frac{1}{2(g-f)} = \frac{1}{g} \tag{8}$$

For susceptibility at Curie point on the unpolarized state, the four-power term $P_a^4 + P_b^4$ is neglected,

$$\chi_{us} = \frac{\Delta P}{\Delta E} = \frac{2}{(2f+g)} = \frac{1}{g} \tag{9}$$

From the results of Eq. (8) and Eq. (9), it clearly shows that the susceptibility is continuous across the Curie point. In other words, the dielectric constant of the

antiferroelectric is continuous across the Curie point if the transition is second order.

Moreover, Kittel developed a first-order transition theory for antiferroelectrics based on Devonshire phase transition theory for FE[16]. Considering the transitions in ferroelectrics, Devonshire treated the transition from the polarized state to the unpolarized state as first order transition as a better way to explain the phenomenon. He gave the free energy function for ferroelectric,

$$A = A_0 + \alpha P^2 + \beta P^4 + \gamma P^6 \tag{10}$$

At the critical point $A = A_0$, the relationships between those variables can be computed as,

$$\begin{cases} P_c^2 = -\dfrac{2\alpha}{\beta} \\ P_c^4 = \dfrac{\alpha}{\gamma} \\ 4\alpha\gamma = \beta^2 \end{cases} \tag{11}$$

Furthermore, the susceptibility of polarized and unpolarized state near the transition temperature is derived as,

$$\chi_{ps} = \frac{1}{8\alpha_c}, \chi_{us} = \frac{1}{2\alpha_c} \tag{12}$$

Apparently, the susceptibility just above the Curie point is four times greater than just below the Curie point,

$$\frac{\chi_{us}}{\chi_{ps}} = 4 \tag{13}$$

This relationship has a good agreement with the experiment results of polycrystalline lead zirconate[22]. The consistency proves that the first order transition theory could be useful in antiferroelectrics. Based on that, Kittel developed a free energy function for the antiferroelectrics system,

$$A = A_0 + f\left(P_a^2 + P_b^2\right) + gP_aP_b + h\left(P_a^4 + P_b^4\right) + j\left(P_a^6 + P_b^6\right) \tag{14}$$

then the first derivative of P_a is expressed as,

$$\frac{\partial A}{\partial P_a} = E = 2fP_a + gP_b + 4hP_a^3 + 6jP_a^5 \tag{15}$$

Without considering the external electric field, the spontaneous polarization ($P_{sa} = -P_{sb}$) in the antiferroelectric state can be derived,

$$6jP_{sa}^4 + 4hP_{sa}^2 + (2f - g) = 0 \tag{16}$$

At the Curie point, the free energy of polarized state should have the same value with unpolarized state that $P_a = P_b = 0$ when,

$$2jP_{sa}^4 + 2hP_{sa}^2 + (2f - g) = 0 \tag{17}$$

The solution of Eq. (16) and Eq. (17) at the Curie point is,

$$P_{sa}^2 = \frac{g - 2f}{h}, \quad P_{sa}^4 = \frac{2f - g}{2j} \tag{18}$$

After that, the susceptibility in antiferroelectric state and unpolarized state at Curie temperature can be obtain,

$$\chi_{as} = \frac{1}{4f - g}, \chi_{us} = \frac{2}{2f + g} \tag{19}$$

Therefore, the results indicate that the susceptibility is discontinuous at the Curie point if the antiferroelectric transition is first order.

To summarize Kittel's work on antiferroelectrics, he is the first person to explain the relationships between susceptibility and the character of transitions. The theory of antiferroelectric phase transition that created by him is fundamental when considering antiferroelectrics.

2.3 Cross' Treatment of Field-Induced Antiferroelectric-to-Ferroelectric Phase Transition

In 1966, L. E. Cross published a paper to investigate the intrinsic switching path for the electric field enforced AFE-to-FE phase transition[23]. He noticed that the thermodynamic instability of the antiferroelectric lattice at high fields is similar to the instability in the paraelectric phase of $BaTiO_3$ by high fields applied just above the Curie point. A simple free energy function of Kittle's crystal is used in Cross's work,

$$G_1 = f\left(P_a^2 + P_b^2\right) + gP_aP_b + h\left(P_a^4 + P_b^4\right) \quad (20)$$

Here, G is the elastic Gibbs function, P_a, P_b are the sub-lattice polarizations and f, g, h are functions dependent on temperature values. For stability, h must be a positive number. Cross rewrote the equation with ferroelectric polarizations $P_F = P_a + P_b$ and antiferroelectric polarizations $P_A = P_a - P_b$,

$$G_1 = \frac{1}{2}\left(f + \frac{g}{2}\right)P_F^2 + \frac{1}{2}\left(f - \frac{g}{2}\right)P_A^2 + \frac{h}{8}\left(P_F^4 + 6P_A^2P_F^2 + P_A^4\right) \quad (21)$$

After applying the external electric field, the switching path can be computed based on the relations between polarization, electric field and the Gibbs free energy. The relations between those variables are obtained according to the minima in the Gibbs free energy at any state of applied field. The computation procedure starts with a specific value of P_F. Thus, the allowed value of P_A can be calculated. Then the corresponding value of E can be derived, consequently, the Gibbs free energy is obtained. The complete switching path can be portrayed by repeating the whole procedure with different initial values of P_F.

By programming on a B 5500 computer, Cross obtained several AFE-to-FE phase

transitions of P-E response under different conditions. The switching curves are similar compared to the experimental switching behavior of $Pb_{0.99}[(Zr_{0.8}Sn_{0.2})_{0.96}Ti_{0.04}]_{0.98}Nb_{0.02}O_3$. Since the thermodynamic functions of the certain material had not been derived, the quantitative comparison for the two results was not achieved. However, Cross successfully provided a method for observation of AFE-to-FE phase transition in a Kittel antiferroelectric.

2.4 Time-dependent Ginzburg-Landau Equation[21]

Previous speculations about Landau-Ginzburg-Devonshire theory only considered a stationary order parameter (polarization). As we would like to study the kinetic phase transition properties, time variation and spatial variation of the polarization should be considered within the GL theory. Thus, the spontaneous polarization moment P(r, t) is a function of spatial position r and time t and the temporal evolutions of the polarization are described by the time dependent Ginzburg-Landau (TDGL) equation[22]:

$$\frac{\partial P(t)}{\partial t} = -L\frac{\partial G}{\partial P(t)} \tag{22}$$

Where L is the kinetic coefficient. The polarization switching process by applying a

time-dependent electric field can be computed from the TDGL equation.

3. Computation

3.1 Algorithm

In this work, the finite difference method and the time dependent Landau-Ginzburg equation are employed to present the computational study of the electric field-induced phase transition in both AFE and FE materials. Typically, the free energy function of a FE single crystal developed by Landau-Ginzburg-Devonshire is introduced for nonlinear polarization behavior of $BaTiO_3$, and the theoretical study of field-induced AFE-to-FE transition is developed based on a simple Kittel AFE model. This section is arranged as follows. Section 3.2 introduces the electric field-induced transition for monolithic materials. For composite materials, the depolarization field effect is considered when computing the switching path, and is detailed introduced in Section 3.3.

3.2 Monolithic Materials

To illustrate the intrinsic nonlinear polarization behavior, single crystals of $BaTiO_3$ and Kittle AFE are considered.

3.2.1 Electric Field-Induced AFE-FE Phase Transition

At this point, our interest is to observe the switching path from AFE to FE under external electric field. In addition, we want to find the requirements for achieving the transition and to investigate how the parameters affect the transition behavior. Following Cross's method and using the time-dependent Landau-Ginzburg equation that was introduced in the previous charpter, the P-E response is derived and detailed introduced in the following way. A simple Kittel AFE model is utilized, with the consideration of external electric field, the free energy function is expressed as

$$G = \frac{1}{2}\left(f + \frac{g}{2}\right)P_F^2 + \frac{1}{2}\left(f - \frac{g}{2}\right)P_A^2 + \frac{h}{8}\left(P_F^4 + 6P_A^2P_F^2 + P_A^4\right) - EP_F \quad (23)$$

where $P_f = P_a + P_b$ and $P_A = P_a - P_b$. Assuming the electric field is zero at the initial state, the values of P_F and P_A can be computed through the minimum free energy. Then, the time-dependent Landau-Ginzburg equation is employed with a slowly increasing external electric field. Both polarization values can be calculated at each time point. Once the maximum electric field is achieved, the same time-dependent Landau-Ginzburg equation is employed with a slightly decreasing electric field. As a consequence, the complete P-E path can be obtained, which is also the switching path of antiferroelectric-ferroelectric transition. According to the time-dependent Landau-

Ginzburg equation,

$$\frac{\partial P}{\partial t} = -L \frac{\partial G}{\partial P} \tag{44}$$

which can be rewritten as,

$$\frac{P' - P}{\Delta t} = -L \frac{\partial G}{\partial P}, \tag{25}$$

Rearranging the order, the polarization at next time step is derived,

$$P' = P - \Delta t \cdot L \frac{\partial G}{\partial P}, \tag{26}$$

where P is the polarization at a certain time point and P' is the polarization after time Δt. Thus, with a sufficient number of evaluations, the polarization for fulfilling the switching path can be obtained by Eq.(26). According to Eq. (23), the first derivative of Gibbs free energy function can be obtained,

$$\frac{\partial G}{\partial P_F} = \left(f + \frac{g}{2}\right)P_F + \frac{3h}{2}P_A^2 P_F + \frac{h}{2}P_F^3 - E \tag{27}$$

and,

$$\frac{\partial G}{\partial P_A} = \left(f - \frac{g}{2}\right)P_A + \frac{3h}{2}P_F^2 P_A + \frac{h}{2}P_A^3 \tag{28}$$

As mentioned before, the values of f, g and h are dependent on temperature. For simplicity, a substitution $g/f = \beta$ is used to make the calculation more convenient. In fact, the values of β have a great impact on the transition behavior, and we will discuss that later. Applying the substitution,

$$\begin{cases} \dfrac{\partial G}{\partial P_F} = \mathrm{f}\left(1 + \dfrac{\beta}{2}\right)P_F + \dfrac{3h}{2}P_A^2 P_F + \dfrac{h}{2}P_F^3 - E \\ \dfrac{\partial G}{\partial P_A} = \mathrm{f}\left(1 - \dfrac{\beta}{2}\right)P_A + \dfrac{3h}{2}P_F^2 P_A + \dfrac{h}{2}P_A^3 \end{cases} \tag{29}$$

To simulate the complete AFE – FE switching path under external electric field, the initial values of P_F and P_A need to be fixed. Nature always prefers the lowest Gibbs free energy, thus, the values of P_F and P_A corresponding to the minima Gibbs free energy can be obtained from the relations,

$$\begin{cases} \dfrac{\partial G}{\partial P_F} = 0 \\ \dfrac{\partial G}{\partial P_A} = 0 \end{cases} \tag{30}$$

The electric field is not applied at the initial state, hence,

$$\frac{\partial G}{\partial P_F} = f\left(1 + \frac{\beta}{2}\right)P_F + \frac{3h}{2}P_A^2 P_F + \frac{h}{2}P_F^3 = 0 \tag{31}$$

$$\frac{\partial G}{\partial P_A} = f\left(1 - \frac{\beta}{2}\right)P_A + \frac{3h}{2}P_F^2 P_A + \frac{h}{2}P_A^3 = 0 \tag{32}$$

Two possible solutions are obtained by solving the equations above，

$$\begin{cases} P_{A0} = 0 \\ P_{F0} = \sqrt{-\dfrac{2f}{h}} \cdot \sqrt{1 + \dfrac{\beta}{2}} \end{cases} \tag{33}$$

and,

$$\begin{cases} P_{A0} = \sqrt{-\frac{2f}{h}} \cdot \sqrt{1-\frac{\beta}{2}} \\ P_{F0} = 0 \end{cases} \tag{34}$$

Both solution (33) and (34) could be the starting point with $E = 0$. It is worth noting that f has to be negative to guarantee the solutions are meaningful. Since both P_{A0} and P_{F0} have the term $\sqrt{-\frac{2f}{h}}$ which can be treated as a constant, to facilitate simulate we assume that

$$P_F = P_{FS}\sqrt{-\frac{2f}{h}} \tag{35}$$

$$P_A = P_{AS}\sqrt{-\frac{2f}{h}} \tag{36}$$

Moreover, to make sure Eq. (35) and Eq. (36) are satisfied, P_a and P_b have to follow the relationship,

$$P_A^2 = -3P_F^2 - \frac{2f}{h}\left(1-\frac{\beta}{2}\right) \tag{37}$$

P_A is meaningful only when the term $-3P_F^2 - \frac{2f}{h}\left(1-\frac{\beta}{2}\right)$ is greater than 0. Taking Eq. (37) into account to solve,

$$-3P_F^2 - \frac{2f}{h}\left(1 - \frac{\beta}{2}\right) \geq 0,$$

$$-3P_{FS}^2\left(-\frac{2f}{h}\right) \geq \frac{2f}{h}\left(1 - \frac{\beta}{2}\right),$$

$$P_{FS}^2 \leq \frac{\left(1 - \frac{\beta}{2}\right)}{3} \tag{38}$$

If P_{FS} is less than $\sqrt{\frac{\left(1 - \beta/2\right)}{3}}$, from Eq. (36), Eq. (37) and Eq. (38),

$$P_{AS}^2\left(-\frac{2f}{h}\right) = -3P_{FS}^2\left(-\frac{2f}{h}\right) + \left(1 - \frac{\beta}{2}\right)\left(-\frac{2f}{h}\right),$$

$$P_{AS} = \sqrt{-3P_{FS}^2 + \left(1 - \frac{\beta}{2}\right)}, \tag{39}$$

Otherwise, P_{AS} is zero. This is an important judging condition in the loop. Then P_{FS} and P_{AS} are applied to the original derivative function,

$$\frac{\partial G}{\partial P_F} = \left[\left(1 + \frac{\beta}{2}\right)P_{FS} - 3P_{AS}^2 P_{FS} - P_{FS}^3 - E\right]\sqrt{-\frac{2f}{h}} \tag{40}$$

where P_{FS}, P_{AS}, and E are the only variables. Thus, the time-dependent Landau-Ginzburg equation can be written as

$$P_{FS}^{'} = P_{FS} - \Delta t \cdot L\left[\left(1 + \frac{\beta}{2}\right)P_{FS} - 3P_{AS}^{2}P_{FS} - P_{FS}^{3} - E\right] \quad (41)$$

During the computation loop, each P_{FS} value will be examined if it satisfies the Eq. (38). Consequently, the new P_{AS} can be determined. Once the new P_{AS} has been calculated, the polarizations at next time step can be calculated according to Eq.(41). Therefore, the full switching path can be observed.

3.2.2 Electric Field-Induced PE-FE Phase Transition

In this work, $BaTiO_3$ is selected as a model system to study the nonlinear polarization behavior associated with the electric field-induced PE-to-FE phase transition. The thermodynamic property of $BaTiO_3$ has been characterized by the following Landau-Ginzburg-Devonshire free energy function[16]:

$$\begin{aligned} G = {} & \alpha_1\left(P_1^2+P_2^2+P_3^2\right)+\alpha_{11}\left(P_1^4+P_2^4+P_3^4\right)+\alpha_{12}\left(P_1^2P_2^2+P_2^2P_3^2+P_3^2P_1^2\right) \\ & +\alpha_{111}\left(P_1^6+P_2^6+P_3^6\right)+\alpha_{112}\left[P_1^4\left(P_2^2+P_3^2\right)+P_2^4\left(P_1^2+P_3^2\right)+P_3^4\left(P_1^2+P_2^2\right)\right] \\ & +\alpha_{123}P_1^2P_2^2P_3^2 \end{aligned} \quad (42)$$

The polynomial coefficients have been experimentally determined[24]: $\alpha_1=3.34*10^5$(T-

381) VmC^{-1}, $\alpha_{11}=4.69*10^6(T-393)-2.02*10^8$ Vm^5C^{-3}, $\alpha_{12}=3.23*10^8$ Vm^5C^{-3}, $\alpha_{111}=-5.52*10^7(T-393) + 2.76*10^9$ Vm^9C^{-5}, $\alpha_{112}=4.47*10^9$ Vm^9C^{-5}, $\alpha_{123}=4.91*10^9$ Vm^9C^{-5}. For convenience, we simplify the Landau-Ginzburg-Devonshire free energy function by considering polarization along P = (P, 0, 0). This becomes

$$G = \alpha_1 P^2 + \alpha_{11} P^4 + \alpha_{111} P^6 - PE \tag{43}$$

Then, $\frac{\partial G}{\partial P}$ is computed,

$$\frac{\partial G}{\partial P} = 2\alpha_1 P + 4\alpha_{11} P^3 + 6\alpha_{111} P^5 - E \tag{44}$$

In this case, the reasonable temperature ranges for an electric-field PE-to-FE phase transition can be determined since all the temperature-dependent variables are known. According to the figure of free energy versus polarization at different temperatures, the characteristic temperatures with different phase stabilities can be determined. Thus, a possible temperature range for field-induced PE-to-FE phase transition can be further estimated. At a certain temperature, α_1, α_{11}, and α_{111} are fixed. Equation (44) can be directly applied to the time-dependent Ginzburg-Landau equation,

$$P' = P - \Delta t \cdot L\left(2\alpha_1 P + 4\alpha_{11}P^3 + 6\alpha_{111}P^5 - E\right) \quad (45)$$

3.3 Composite Materials

For wide application in various areas, polymer-matrix composites with active functional fillers have been important alternatives to monolithic inorganic materials. In this case, ferroelectric ceramic particle-filled polymer-matrix composites gives unique properties that conventional single-component ferroelectric materials cannot offer[25].

3.3.1 Depolarization Field E_d and Depolarization Factor L

In composite materials where a ferroelectric layer is inserted between two polymers (or two conducting electrodes), the polarization charges are induced at the inside surface of the ferroelectric layer when external electric field is applied. Thus, the compensated charges will be induced at the outside surface of the ferroelectric layer due to the free charge carriers in the polymers. However, in reality the compensated charge is finite due to the screening length λ[26]. This imperfect charge compensation could induce a depolarization field has an opposite direction with the ferroelectric polarization, which is also the main reason for the dependence of the ferroelectric polarization on the thickness of the ferroelectric film[27]. Therefore, the influence of depolarization field

effect on the ferroelectric behavior is investigated.

To quantize the relationship between depolarization field and polarization, depolarization factor L is introduced by[28],

$$E_d = \frac{L}{\varepsilon_0} P \tag{46}$$

Where ε_0 is the permittivity of free space. The depolarization factor is independent of the volume of the dielectric and mainly related to the shape of the dielectric. Wang et al. [25, 29]has simulated the macroscopic properties of composites containing ferroelectric particles and proved that the depolarization factor is more sensitive to the arrangement and connectivity of the ferroelectric particles.

Considering a sphere dielectric, the inside electric potential can be calculated according to Laplace's equation and boundary conditions. Then the depolarization factors along three orthogonal axis a, b and c direction is given by[28]

$$
\begin{aligned}
L_a &= \frac{abc}{2}\int_0^{\infty}\frac{1}{\left(s+a^2\right)R_s}\,ds \\
L_b &= \frac{abc}{2}\int_0^{\infty}\frac{1}{\left(s+b^2\right)R_s}\,ds \\
L_c &= \frac{abc}{2}\int_0^{\infty}\frac{1}{\left(s+c^2\right)R_s}\,ds
\end{aligned}
\tag{47}
$$

where $R_s = \sqrt{\left(s+a^2\right)+\left(s+b^2\right)+\left(s+c^2\right)}$ and s is an integration variable. In a sphere dielectric, the three depolarization factors are equal, $L_a = L_b = L_c = 1/3$. From Eq.(47), we can also prove that the depolarization factor is dependent on the shape of the dielectric. Depolarization factors in some special cases are summarized in Table 1.

Table 1 Depolarization factors in spectial cases

Shape of dielectric	**Thin film**	**Thin film**	**Long cylinder**	**Long cylinder**
External electric field direction	Vertical	Parallel	Parallel to axis	Vertical to axis
Depolarization factor	1	0	0	0.5

3.3.2 Particle-Filled Polymer-Matrix Composite for AFE/PE-FE Phase Transition

In last section, the depolarization field E_d and depolarization factor L is introduced. The

linear relationship between depolarization field E_d and polarization P is shown in Fig. (4).

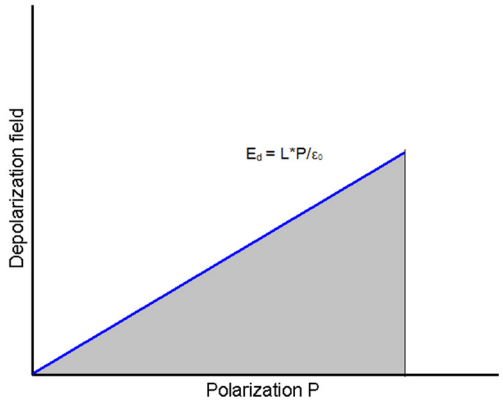

Figure 4 Depolarization field versus polarization to obtain the free energy of E_d

Thus, the free energy of depolarization field can be expressed as

$$G_d = \frac{L}{2\varepsilon_0} P^2 \tag{48}$$

It is worth noting that E_d is in the opposite direction of external electric field E, a resistance to the polarization.

For AFE-to-FE phase transition model, the free energy of depolarization field is considered in the total free energy function,

$$G = \frac{1}{2} f\left(1 + \frac{\beta}{2}\right) P_F^2 + \frac{1}{2} f\left(1 - \frac{\beta}{2}\right) P_A^2 + \frac{h}{8}\left(P_F^4 + 6P_A^2 P_F^2 + P_A^4\right) - EP_F + \frac{L}{2\varepsilon_0} P_F^2$$

(49)

then,

$$\frac{\partial G}{\partial P_F} = \left[\left(1 + \frac{\beta}{2}\right) P_{FS} - 3P_{AS}^2 P_{FS} - P_{FS}^3 - E + \frac{L}{\varepsilon_0} P_{FS}\right] \sqrt{-\frac{2f}{h}} \qquad (50)$$

The new P_F after applying the time-dependent Ginzburg-Landau equation is

$$P_{FS}^{'} = P_{FS} - \Delta t \cdot L^{*}\left[\left(1 + \frac{\beta}{2}\right) P_{FS} - 3P_{AS}^2 P_{FS} - P_{FS}^3 - E + \frac{L}{\varepsilon_0} P_{FS}\right] \qquad (51)$$

Where the L^* is the kinetic coefficient. Similarly, we modify our model for PE-FE phase transition in the same way. According to (49) we have,

$$G = \alpha_1 P^2 + \alpha_{11} P^4 + \alpha_{111} P^6 - PE + \frac{L}{2\varepsilon_0} P^2 \qquad (52)$$

Then,

$$\frac{\partial G}{\partial P} = 2\alpha_1 P + 4\alpha_{11} P^3 + 6\alpha_{111} P^5 - E + \frac{L}{\varepsilon_0} P \tag{53}$$

$$P' = P - \Delta t \cdot L \left(2\alpha_1 P + 4\alpha_{11} P^3 + 6\alpha_{111} P^5 - E + \frac{L}{\varepsilon_0} P \right) \tag{54}$$

Thus, the depolarization field has been added into both our models. The spatial-temporal evolution of the ferroelectric polarization in response to varying electric field under depolarization field can be computed.

4. Results

The computation for the phase switching path was programmed for an IBM ThinkPad E531 computer. The appropriate values of all the parameters for getting meaningful results have been confirmed after continuous testing. The parameters of AFE-FE phase transition are different from PE-FE phase transition since the unit is unknown. The kinetic coefficient L is 10^{-3} and delta t is 1 for AFE-FE transition. For PE-FE transition, L was chosen to be 10^{-8} and delta t kept the same.

4.1 Electric Field-Induced AFE-FE Phase Transition

Before we start the computation for the antiferroelectric to ferroelectric phase transition, we have to unify the units since all the functions involve the constants in the initial energy function (f, g, h). Based on chapter 3, we have summarized the units of our variables as in Table 2.

Table 2 Units for several parameters

Parameter	**Free enegery**	**FE polarization**	**AFE polarization**	**Electric field**	**Depolarization Factor**
Notation	**G**	$\mathbf{P_F}$	$\mathbf{P_A}$	**E**	**L**
unit	$\frac{f^2}{2\mathrm{h}}$	$\sqrt{-\frac{2f}{\mathrm{h}}}$	$\sqrt{-\frac{2f}{\mathrm{h}}}$	$\sqrt{-\frac{2f^3}{\mathrm{h}}}$	$f\,\frac{\mathrm{F}}{\mathrm{m}}$

4.1.1 Monolithic AFE Materials

The whole computation was repeated for different β values, each time have run for 300000 steps. The corresponding P-E response is shown in Figs. (5) and (6).

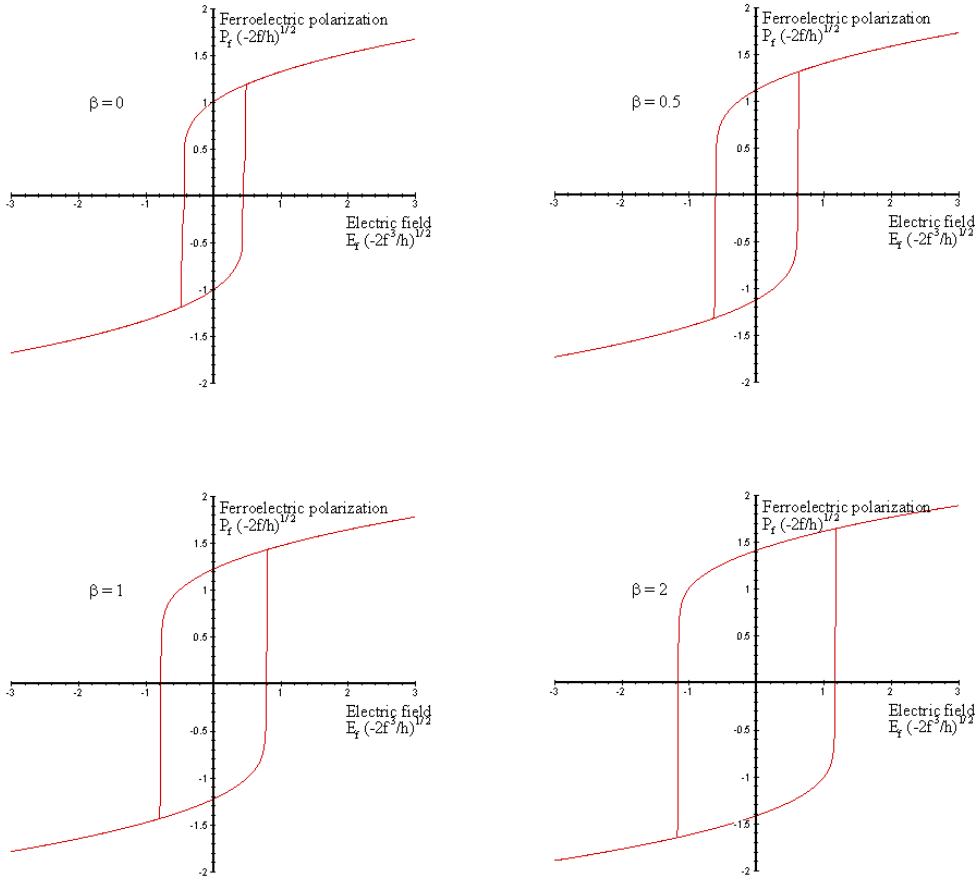

Figure 5 P-E response for several positive β values

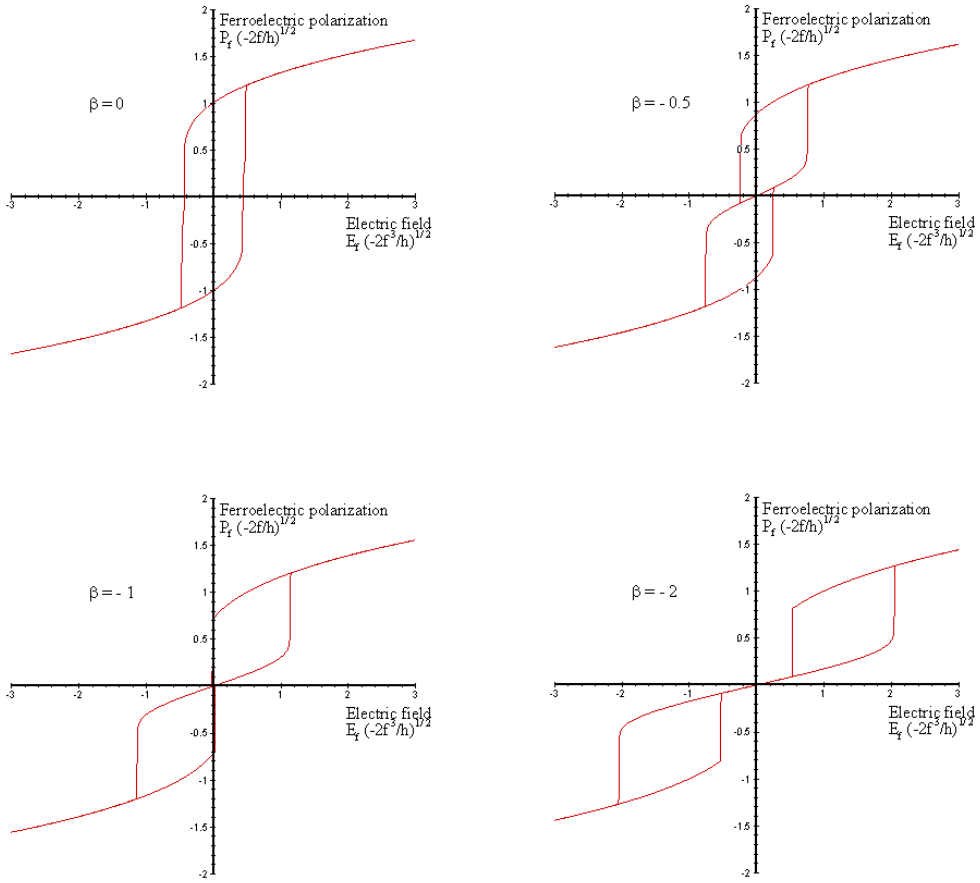

Figure 6 P-E response for several negative β values

In Fig. (5), the computation starts at $P_{A0} = 0$, $P_{F0} = \sqrt{1 + \frac{\beta}{2}}$ because β has a positive value. The switching path indicates that the ferroelectric phase is very stable and the antiferroelectric phase is instable. However, for negative β values shown in Fig. (6), the hysteresis loops have the tendency to separate into two full hysteresis loop which is caused by the electric field-induced antiferroelectric to ferroelectric phase transition.

When 0>β>-1, the antiferroelectric phase is stable and the ferroelectric phase is metastable which gives rise to the kinks of the hysteresis. The formation of two full hysteresis loops are completed for those β that are smaller than -1, since then, the antiferroelectric phase is stable and the ferroelectric phase is instable but can be induced by the electric field. Moreover, there will be no residual polarization because the polarization will spontaneously disappear upon removal of electric field, which allows it to release the stored energy.

4.1.2 AFE Particle-Filled Polymer-Matrix Composite

In this work, we added the depolarization field to the free energy function to investigate the P-E response of the particle-filled polymer-matrix composite. It is worth noting that temperature is not a parameter in our computations, but in reality T would enter through the constant f, g and h as we have mentioned before. Here we choose β = -2 as a reference since it shows the obvious AFE to FE transition. The electric field-induced AFE-to-FE phase transition for different depolarization factors is accompanied by hysteresis as detailed in Fig. (7) and Fig. (8).

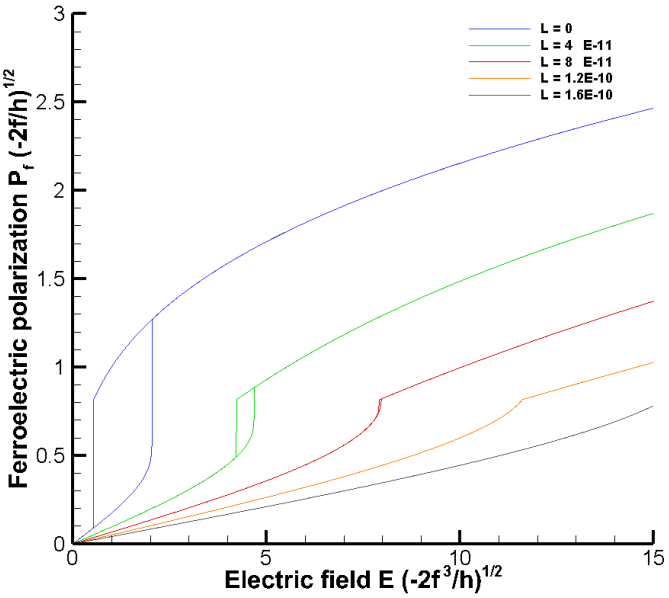

Figure 7 P-E response with different depolarization factors (β =-2)

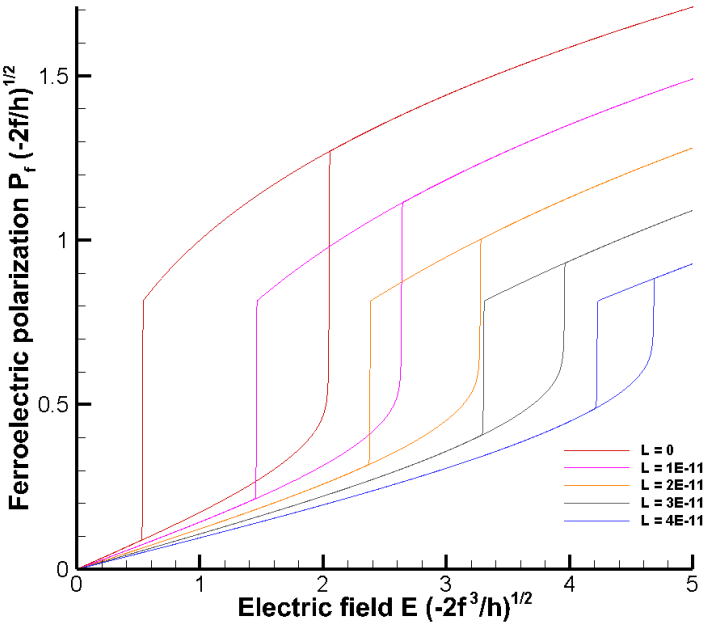

Figure 8 P-E response for small depolarization factors (β =-2)

We extended the maximum electric field by increasing the steps to 1500000 for observing the trend of the switching path. The hysteresis gradually shrunk with the growth of depolarization factor L, eventually becoming a straight line. Detailed P-E response changes with lower depolarization factor is shown in Fig. (8). The result clearly shows that depolarization field is a hindrance to the electric-field induced AFE-FE transition. A small depolarization factor can have a large impact on the dielectric properties of an antiferroelectric composite.

4.2 Electric Field-Induced PE-FE Phase Transition

4.2.1 $BaTiO_3$ Single Crystal

To illustrate the intrinsic dielectric behavior of $BaTiO_3$ single crystal, we plot the Landau-Ginzburg-Devonshire free energy as a function of polarization along [100] direction at different temperatures in Fig. (9).

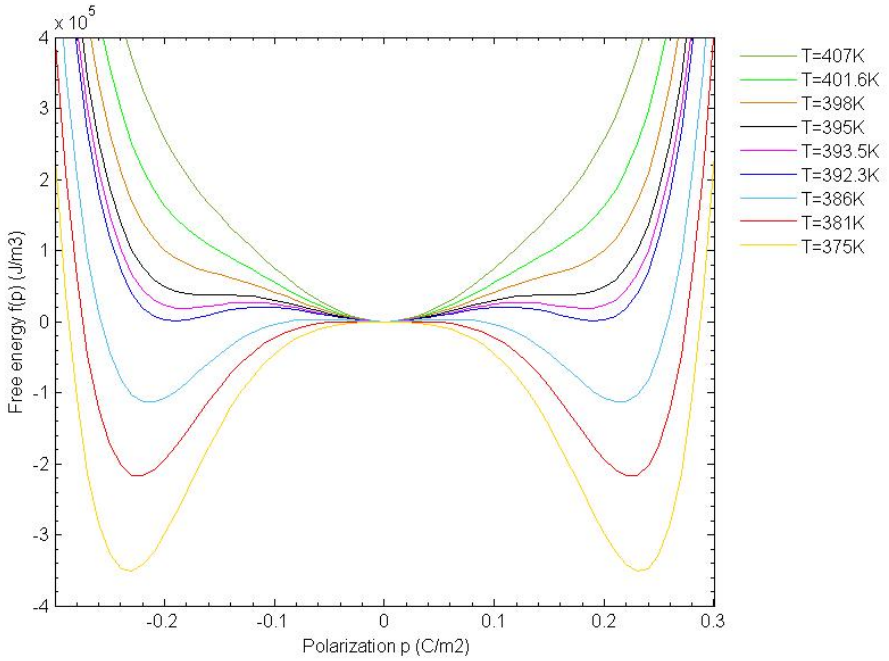

Figure 9 Landau-Ginzburg-Devonshire free energy f (p) as a function of polarization along p= (p, 0, 0) at different temperature

According to Fig. (9), four characteristic temperatures can be defined. T_0 is the Curie-Weiss temperature, T_c is the Curie temperature where paraelectric and ferroelectric phase have equal free energy, and T_1 and T_2 are the boundary temperature that a paraelectric to ferroelectric phase transition will occur by an applying external electric field. Explicit relationships between temperature and phase stabilities are indicated in Table 3,

Table 3Phase stabilities at different temperature

Temperature range	$T < T_0$	$T_0 < T < T_C$	$T_C < T < T_1$	$T_1 < T < T_2$	$T_2 < T$
PE phase	Instable	Metastable	Stable	Stable	Stable
FE phase	Stable	Stable	Metastable	Instable	Instable

Based on the information in Table 3, we have illustrated that the electric-field induced paraelectric to ferroelectric phase transition could happen from 395K to 401.6K. Furthermore, we have captured the hysteresis loop at different temperatures to demonstrate that the paraelectric to ferroelectric phase transition can be induced by external electric field only at certain temperature ranges.

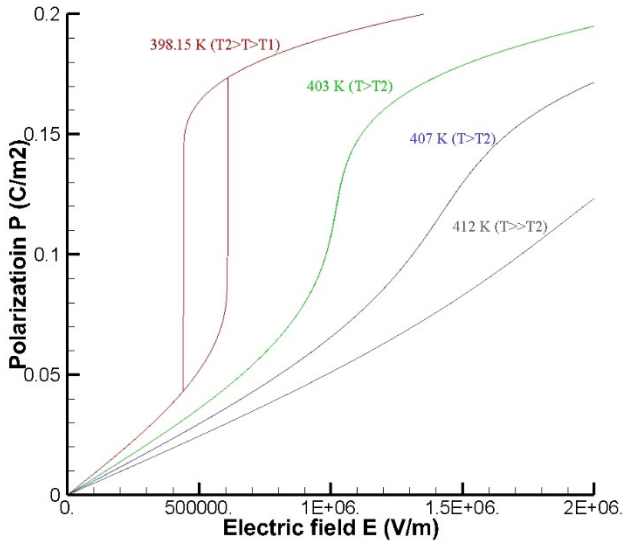

Figure 10 Polarization-electric field (P-E) response at different temperatures along [100]

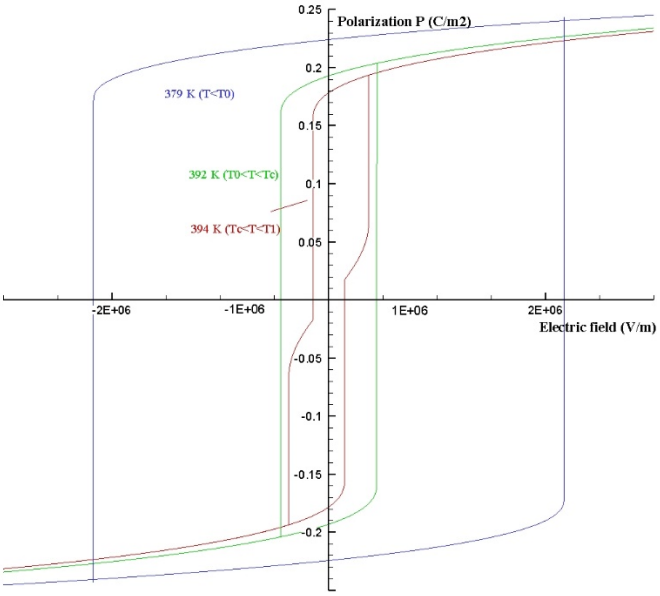

Figure 11 Polarization-electric field (P-E) response at different temperatures along [100]

Figures (10) and (11) show different P-E responses at different temperature ranges when an external electric field is applied along [100] direction. We can clearly indicate that the barium titanate is a standard ferroelectric with large hysteresis at temperature lower than T_0 = 381K. The hysteresis loop becomes smaller at temperature range from T_0 to T_C but the ferroelectric phase is still stable. When temperature is higher than the Curie point but lower than T_1, the paraelectric phase is stable but ferroelectric phase is metastable. The kinks of the hysteresis loop are caused by the electric field-induced paraelectric to ferroelectric phase transition, but the polarization does not return to zero even after the electric field is removed as long as temperature is lower than T_1. The

ferroelectric phase is instable but can be induced by the electric field when we increase the temperature to next temperature range. Moreover, at temperature higher than T_1, the polarization will spotenously return to zero once the external electric field is removed like AFE-FE transition. The electric field-induced paraelectric to ferroelectric phase transition will no longer exist when temperature is higher than T_2. If we keep increasing the temperature the *P-E* response will eventually be linearly dependent. Thus, we consider temperature between T_1 and T_2 to observe the electric field-induced paraelectric to ferroelectric phase transition.

4.2.2 $BaTiO_3$ Particle-Filled Polymer-Matrix Composite

To investigate the depolarization field influence on such phase transition behavior, *P-E* responses at different depolarization factors is shown in Fig. (12).

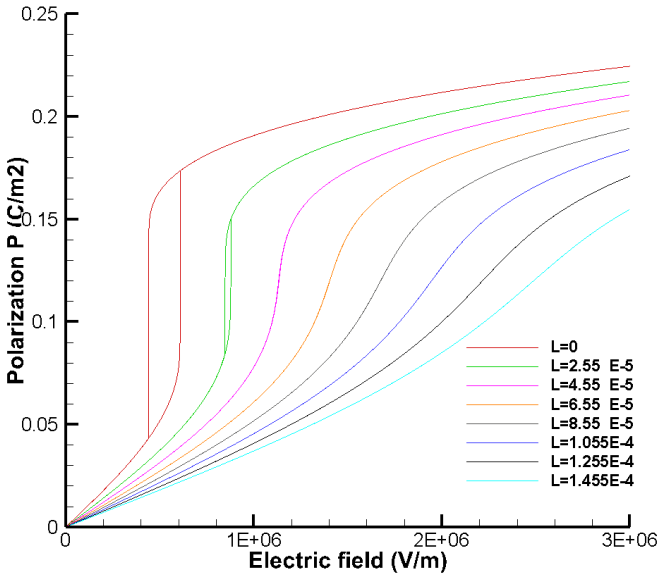

Figure 12 P-E response with different depolarization factor values (T=398.15K)

The results are similar to the AFE-FE transition. It clearly shows that the PE to FE phase transition will gradually disappear following the increasing depolarization factor. From the trend of the curve, we can indicate that eventually the P-E response will turn into a simple straight line. When L approaches a value of 1, the dielectric can be treated like an infinite long film which is vertical to the external electric field. Thus, the compensated field can perfectly counteract the inside polarization and this is the reason why it has linear relationship. The detailed P-E dependence on low depolarization factors is shown in Fig. (13).

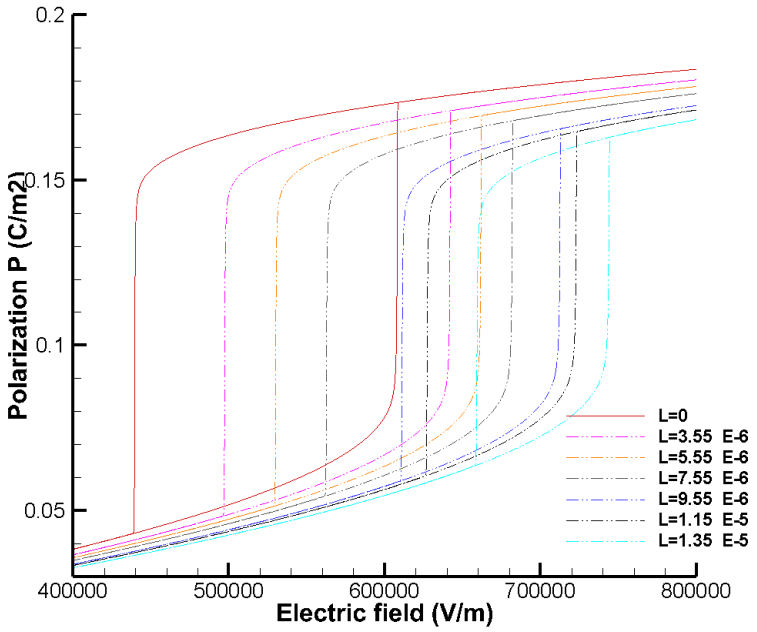

Figure 13 P-E response for small depolarization factor (T=398.15K)

5. Conclusion

Based on Kittel simple antiferroelectric model and a time-dependent Ginzburg-Landau equation, we have successfully revealed the switching path of electric field-induced AFE-to-FE transition. Similar results of electric field-induced PE-FE transition have been obtained in a $BaTiO_3$ single crystal system. These special double hysteresis loops show a larger width than conventional ferroelectric materials. Furthermore, the polarization will spontaneously return back to zero once the electric field goes to zero. This kind of dielectric property response demonstrates that materials with an electric

field-induced AFE/PE-to-FE phase transitions are capable for high energy density capacitors.

A particle-filled polymer-matrix composite consisting of these kind of materials has been examined through considering the internal depolarization field. We have demonstrated that the depolarization field is an obstacle to the AFE/PE-to-FE phase transition. The hysteresis loop gradually disappears with the increasing of depolarization factors. Moreover, a small depolarization factor can completely prevent the AFE/PE-FE transition, noting that the shape and alignment of the AFE/FE particles embedded in a polymer matrix are essential to the dielectric properties of the composites.

6. References

1. Chauhan, A., et al., *Anti-Ferroelectric Ceramics for High Energy Density Capacitors.* Materials, 2015. **8**(12).
2. Gorzkowski, E.P., et al., *Glass-ceramics of barium strontium titanate for high energy density capacitors.* Journal of Electroceramics, 2007. **18**(3): p. 269-276.
3. Ortega, N., et al., *Relaxor-ferroelectric superlattices: high energy density capacitors.* Journal of Physics: Condensed Matter, 2012. **24**(44): p. 445901.
4. Valasek, J., *Piezo-electric and allied phenomena in Rochelle salt.* Physical review, 1921. **17**(4): p. 475.
5. Von Hippel, A., *Ferroelectricity, domain structure, and phase transitions of barium titanate.* Reviews of Modern Physics, 1950. **22**(3): p. 221.
6. Castelli, I.E. and K.W. Jacobsen, *Designing rules and probabilistic weighting for fast materials discovery in the Perovskite structure.* Modelling and Simulation in Materials Science and

Engineering, 2014. **22**(5): p. 055007.
7. Kresin, V.Z. and W. Knight, *Pair Correlations in Many-Fermion Systems*. 1998: Springer.
8. Strukov, B.A. and A.P. Levanyuk, *Ferroelectric phenomena in crystals: physical foundations*. 2012: Springer Science & Business Media.
9. Kittel, C., *Theory of Antiferroelectric Crystals.* Physical Review, 1951. **82**(5): p. 729-732.
10. Pulvari, C.F., *Ferrielectricity.* Physical Review, 1960. **120**(5): p. 1670-1673.
11. Hao, X., et al., *A comprehensive review on the progress of lead zirconate-based antiferroelectric materials.* Progress in Materials Science, 2014. **63**: p. 1-57.
12. Bowen, C.R., et al., *Piezoelectric and ferroelectric materials and structures for energy harvesting applications.* Energy & Environmental Science, 2014. **7**(1): p. 25-44.
13. Bharadwaja, S.S.N., et al., *ac transport studies of La-modified antiferroelectric lead zirconate thin films.* Physical Review B, 2002. **65**(17): p. 174106.
14. Satyanarayan, P., C. Aditya, and V. Rahul, *Enhancing electrical energy storage density in anti-ferroelectric ceramics using ferroelastic domain switching.* Materials Research Express, 2014. **1**(4): p. 045502.
15. Satyanarayan, P., C. Aditya, and V. Rahul, *A technique for giant mechanical energy harvesting using ferroelectric/antiferroelectric materials.* J. Appl. Phys, 2014. **115**: p. 084908.
16. Devonshire, A.F., *XCVI. Theory of barium titanate.* Philosophical Magazine and Journal of Science, 1949. **40**(309).
17. Olmster, P.D., *Lectures on Landau Theory of Phase Transitions*. 2000, Department of Physics and Astronomy: University of Leeds.
18. Chandra, P. and P.B. Littlewood, *A Landau Primer for Ferroelectrics*, in *Physics of Ferroelectrics: A Modern Perspective*. 2007, Springer Berlin Heidelberg: Berlin, Heidelberg. p. 69-116.
19. Valasek, J., *Piezo-Electric and Allied Phenomena in Rochelle Salt.* Physical Review, 1921. **17**(4): p. 475-481.
20. Fridkin, V. and S. Ducharme, *Ferroelectricity at the nanoscale: basics and applications*. 1 ed. 2014: Springer-Verlag Berlin Heidelberg. XII, 122.
21. Ginzburg, V.L., Zh. Eksp. Teor. Fiz., 1945. **15**(739).
22. Shirane, G., E. Sawaguchi, and A. Takeda, *On the Phase Transition in Lead Zirconate.* Physical Review, 1950. **80**(3): p. 485-485.
23. Cross, L.E., *Antiferroelectric-Ferroelectric Switching in a Simple "Kittel" Antiferroelectric.* Journal of the Physical Society of Japan, 1967. **23**(1): p. 77-82.
24. Bell, A., *Phenomenologically derived electric field-temperature phase diagrams and piezoelectric coefficients for single crystal barium titanate under fields along different axes.* Journal of Applied Physics, 2001. **89**(7): p. 3907-3914.
25. Ma, F.D. and Y.U. Wang, *Depolarization field effect on dielectric and piezoelectric properties of particulate ferroelectric ceramic-polymer composites.* Journal of Applied Physics, 2015. **117**(12): p. 124101.
26. Kim, D.J., et al., *Polarization Relaxation Induced by a Depolarization Field in Ultrathin*

Ferroelectric ${\mathrm{BaTiO}}_{3}$ Capacitors. Physical Review Letters, 2005. **95**(23): p. 237602.

27. Pertsev, N. and H. Kohlstedt, *Depolarizing-field effect in strained nanoscale ferroelectric capacitors and tunnel junctions.* arXiv preprint cond-mat/0603762, 2006.
28. Dong, W., *THE DEPOLARIZATION FACTOR.* 2003.
29. Wang, Y.U. and D.Q. Tan, *Computational study of filler microstructure and effective property relations in dielectric composites.* Journal of Applied Physics, 2011. **109**(10): p. 104102.

Appendix A: C++ Code for AFE-to-FE Phase Transition (Monolithic)

```
#include <fstream>
#include <sstream>
#include <iostream>
#include <string>
#include <vector>
#include <map>
#include <time.h>
#include <math.h>
using namespace std;
#define L      0.001            //delat t
#define K      1
#define n 300000              //Steps
#define T 398.15             //Temperature
double p0[n];
double e0[n];
double p1[2 * n];
double e1[2 * n];
double p2[n];
double e2[n];
double pa0[n];
double pa1[n];
double pa2[n];
double p3[n];
double e3[n];
double pa3[n];
double n2 = n * 2;
double beta = -1;
double f = -1;
double Pf0, Pa0, Pf1, Pf10, Pa10, Pf2, Pf20, Pa20, Pa1, Pa2, Eone, E2;
double Pf = 0, Pa = sqrt(1 - beta / 2), E = 0;
```

```
double get_power_res(double x_, int n_){
	double res = x_;
	for (int i = 0; i < n_ - 1; i++){
		res = res*x_;
	}
	return res;
}

double func1(){
	int	i = 0;
	while (i < n){
		p0[i] = Pf;
		e0[i] = E;
		pa0[i] = Pa;
		Pf0 = Pf - L*f*((1 + beta / 2)*Pf - 3 * Pa*Pa*Pf - Pf*Pf*Pf - E);
		if (Pf*Pf>(1 - beta / 2) / 3){
			Pa = 0;
		}
		else{
			Pa = sqrt(-3 * Pf*Pf + 1 - beta / 2);
		}
		E += 0.00001;
		Pf = Pf0;
		i++;
	}

	int	k = 0;
	while (k<n) {
		p1[k] = Pf;
		e1[k] = E;
		pa1[k] = Pa;
		Pf0 = Pf - L*f*((1 + beta / 2)*Pf - 3 * Pa*Pa*Pf - Pf*Pf*Pf - E);
		if (Pf*Pf>(1 - beta / 2) / 3){
			Pa = 0;
		}
		else{
			Pa = sqrt(-3 * Pf*Pf + 1 - beta / 2);
		}
```

```
        E -= 0.00001;
        Pf = Pf0;
        k++;
    }
    int    j = 0;
    while (j<n) {
        p2[j] = Pf;
        e2[j] = E;
        pa2[j] = Pa;
        Pf0 = Pf - L*f*((1 + beta / 2)*Pf - 3 * Pa*Pa*Pf - Pf*Pf*Pf - E);
        if (Pf*Pf>(1 - beta / 2) / 3){
            Pa = 0;
        }
        else{
            Pa = sqrt(-3 * Pf*Pf + 1 - beta / 2);
        }
        E -= 0.00001;
        Pf = Pf0;
        j++;
    }
    int    c = 0;
    while (c<n) {
        p3[c] = Pf;
        e3[c] = E;
        pa3[c] = Pa;
        Pf0 = Pf - L*f*((1 + beta / 2)*Pf - 3 * Pa*Pa*Pf - Pf*Pf*Pf - E);
        if (Pf*Pf>(1 - beta / 2) / 3){
            Pa = 0;
        }
        else{
            Pa = sqrt(-3 * Pf*Pf + 1 - beta / 2);
        }
        E += 0.00001;
        Pf = Pf0;
        c++;
    }
    return E;
}
```

```
int main(){
	func1();
	char fname[100];
	fstream file;
	string delimiter = ",";
	string filename;
	string file_dir = "C:\\Users\\sumyuri\\Desktop\\research\\newdata\\";
	stringstream ss;
	ss << beta;
	filename = ss.str();
	string str_file = file_dir + filename + ".dat";
	sprintf_s(fname, str_file.c_str());
	file.open(fname, ios_base::out);
	file << "TITLE= \"polarization\"" << endl
		<< "VARIABLES = \"E\", \"P\"" << endl
		<< "ZONE T=\"zone\" DATAPACKING=POINT" << endl
		<< endl;
	for (int i = 0; i < n; i++){
		file << e0[i] << delimiter
			<< p0[i] << delimiter
			<< endl;
	}
	for (int k = 0; k < n; k++){
		file << e1[k] << delimiter
			<< p1[k] << delimiter
			<< endl;
	}
	for (int j = 0; j < n; j++){
		file << e2[j] << delimiter
			<< p2[j] << delimiter
			<< endl;
	}
	for (int c = 0; c < n; c++){
		file << e3[c] << delimiter
			<< p3[c] << delimiter
			<< endl;
	}
	file.close();
	return 0;
```

}

Appendix B: C++ Code for AFE-to-FE Phase Transition (Composite)

```
#include <fstream>
#include <sstream>
#include <iostream>
#include <string>
#include <vector>
#include <map>
#include <time.h>
#include <math.h>
using namespace std;
#define L     0.001          //delat t
#define K     1
#define n 500000             //Steps
double p0[n];
double e0[n];
double p1[2 * n];
double e1[2 * n];
double p2[n];
double e2[n];
double pa0[n];
double pa1[n];
double pa2[n];
double p3[n];
double e3[n];
double pa3[n];
double n2 = n * 2;
double beta = -2;
double f = -1;
double Pf0, Pa0, Pf1, Pf10, Pa10, Pf2, Pf20, Pa20, Pa1, Pa2, Eone, E2;
double Pf = 0, Pa = sqrt(1 - beta / 2),E=0;
double D = 0; //0.00000000008;
double e00 = 8.85/1e12;
```

```
double get_power_res(double x_, int n_){
	double res = x_;
	for (int i = 0; i < n_ - 1; i++){
		res = res*x_;
	}
	return res;
}
double func1(){
	int	i = 0;
	while (i < n){
		p0[i] = Pf;
		e0[i] = E;
		pa0[i] = Pa;
		Pf0 = Pf - L*f*((1 + beta / 2)*Pf - 3 * Pa*Pa*Pf - Pf*Pf*Pf + E - D*Pf/e00);
		if (Pf*Pf>(1 - beta / 2) / 3){
			Pa = 0;
		}
		else{
			Pa = sqrt(-3 * Pf*Pf + 1 - beta / 2);
		}
		E += 0.00001;
		Pf = Pf0;
		i++;
	}
	int	k = 0;
	while (k<n) {
		p1[k] = Pf;
		e1[k] = E;
		pa1[k] = Pa;
		Pf0 = Pf - L*f*((1 + beta / 2)*Pf - 3 * Pa*Pa*Pf - Pf*Pf*Pf + E - D*Pf/e00);
		if (Pf*Pf>(1 - beta / 2) / 3){
			Pa = 0;
		}
		else{
			Pa = sqrt(-3 * Pf*Pf + 1 - beta / 2);
		}
		E -= 0.00001;
		Pf = Pf0;
```

```
        k++;
    }
    /*int    j = 0;
    while (j<n) {
        p2[j] = Pf;
        e2[j] = E;
        pa2[j] = Pa;
        Pf0 = Pf - L*f*((1 + beta / 2)*Pf - 3 * Pa*Pa*Pf - Pf*Pf*Pf + E);
        if (Pf*Pf>(1 - beta / 2) / 3){
            Pa = 0;
        }
        else{
            Pa = sqrt(-3 * Pf*Pf + 1 - beta / 2);
        }
        E += 0.00001;
        Pf = Pf0;
        j++;
    }
    int    c = 0;
    while (c<n) {
        p3[c] = Pf;
        e3[c] = E;
        pa3[c] = Pa;
        Pf0 = Pf - L*f*((1 + beta / 2)*Pf - 3 * Pa*Pa*Pf - Pf*Pf*Pf + E);
        if (Pf*Pf>(1 - beta / 2) / 3){
            Pa = 0;
        }
        else{
            Pa = sqrt(-3 * Pf*Pf + 1 - beta / 2);
        }
        E -= 0.00001;
        Pf = Pf0;
        c++;
    }*/
    return E;
}

int main(){
    func1();
```

```
char fname[100];
fstream file;
string delimiter = ",";
string filename;
string filename2;
string file_dir = "C:\\Users\\sumyuri\\Desktop\\research\\antiferrodata\\";
stringstream ss;
stringstream bb;
bb << D;
ss << beta;
filename = ss.str();
filename2 = bb.str();
string str_file = file_dir + filename + "+" +filename2+ ".dat";
sprintf_s(fname, str_file.c_str());
file.open(fname, ios_base::out);
file << "TITLE= \"polarization\"" << endl
     << "VARIABLES = \"E\", \"P\"" << endl
     << "ZONE T=\"zone\" DATAPACKING=POINT" << endl
     << endl;
for (int i = 0; i < n; i++){
     file << e0[i] << delimiter
          << p0[i] << delimiter
          << endl;
}
for (int k = 0; k < n; k++){
     file << e1[k] << delimiter
          << p1[k] << delimiter
          << endl;
}
/*for (int j = 0; j < n; j++){
     file << e2[j] << delimiter
          << p2[j] << delimiter
          << endl;
}
for (int c = 0; c < n; c++){
     file << e3[c] << delimiter
          << p3[c] << delimiter
          << endl;
}*/
```

```
	file.close();
	return 0;
}
```

Appendix C: C++ Code for PE-to-FE Phase Transition (Monolithic)

```
#include <fstream>
#include <sstream>
#include <iostream>
#include <string>
#include <vector>
#include <map>
#include <time.h>
#include <math.h>
using namespace std;
#define L	1/1E8		//delat t
#define K	1
#define n 300000		//Steps
#define T 394		//Temperature
double a = 3.34E5*(T - 381);			//alpha1
double aa = 4.69E6*(T - 393) - 2.02E8;		//alpha11
double aaa = -5.52E7*(T - 393) + 2.76E9;	//alpha111
double ab = 3.23E8;
double aab = 4.47E9;
double abc = 4.91E9;
double p1[n], p2[n], p3[n], p4[n];
double e1[n], e2[n], e3[n], e4[n];
double Pa0, Ma0, Na;
double Pa = 0.178, Ea = 0;

double get_power_res(double x_, int n_){
	double res = x_;
	for (int i = 0; i < n_ - 1; i++){
		res = res*x_;
	}
```

```
    return res;
}

double func1(){

    int counter = 0, i = 0;
    while (i < n){
        p1[i] = Pa;
        e1[i] = Ea;
        Pa0 = Pa - L*K*(2 * a*Pa + 4 * aa*get_power_res(Pa, 3) + 6 *
aaa*get_power_res(Pa, 5) - Ea );
        Ea -= 10;
        Pa = Pa0;
        i++;
    }
    int w = 0;
    while (w < n){
        p2[w] = Pa;
        e2[w] = Ea;
        Pa0 = Pa - L*K*(2 * a*Pa + 4 * aa*get_power_res(Pa, 3) + 6 *
aaa*get_power_res(Pa, 5) - Ea );
        Ea += 10;
        Pa = Pa0;
        w++;
    }
    int r = 0;
    while (r < n){
        p3[r] = Pa;
        e3[r] = Ea;
        Pa0 = Pa - L*K*(2 * a*Pa + 4 * aa*get_power_res(Pa, 3) + 6 *
aaa*get_power_res(Pa, 5) - Ea );
        Ea += 10;
        Pa = Pa0;
        r++;
    }
    int y = 0;
    while (y < n){
        p4[y] = Pa;
        e4[y] = Ea;
```

```
        Pa0 = Pa - L*K*(2 * a*Pa + 4 * aa*get_power_res(Pa, 3) + 6 *
aaa*get_power_res(Pa, 5) - Ea );
        Ea -= 10;
        Pa = Pa0;
        y++;
    }
    return 0;
}

int main(){
    func1();
    char fname[100];
    fstream file;
    string delimiter = ",";
    string filename;
    string filename2;
    string file_dir = "C:\\Users\\sumyuri\\Desktop\\research\\normalPEFEdata\\";
    stringstream ss;
    stringstream bb;
    ss << T;
    bb << D;
    filename = ss.str();
    filename2 = bb.str();
    string str_file = file_dir + filename + "+" + filename2 + ".dat";
    sprintf_s(fname, str_file.c_str());
    file.open(fname, ios_base::out);
    file << "TITLE= \"polarization\"" << endl
        << "VARIABLES = \"E\", \"P\"" << endl
        << "ZONE T=\"zone\" DATAPACKING=POINT" << endl
        << endl;
    for (int i = 0; i < n; i++){
        file << e1[i] << delimiter
            << p1[i] << delimiter
            << endl;
    }
    for (int w = 0; w < n; w++){
        file << e2[w] << delimiter
            << p2[w] << delimiter
            << endl;
```

```
        }
        for (int r = 0; r < n; r++){
            file << e3[r] << delimiter
                 << p3[r] << delimiter
                 << endl;
        }
        for (int y = 0; y < n; y++){
            file << e4[y] << delimiter
                 << p4[y] << delimiter
                 << endl;
        }
        file.close();
        return 0;
}
```

Appendix D: C++ Code for PE-to-FE Phase Transition (Composite)

```
#include <fstream>
#include <sstream>
#include <iostream>
#include <string>
#include <vector>
#include <map>
#include <time.h>
#include <math.h>
using namespace std;
#define L     1/1E8             //delat t
#define K     1
#define n 100000                  //Steps
#define T 398.15             //Temperature
#define D 0.0000135
double a = 3.34E5*(T - 381);                    //alpha1
double aa = 4.69E6*(T - 393) - 2.02E8;       //alpha11
double aaa = -5.52E7*(T - 393) + 2.76E9;     //alpha111
double ab = 3.23E8;
double aab = 4.47E9;
double abc = 4.91E9;
double p1[n], p11[n];
double e1[n], e11[n];
double Pa0, Ma0, Na;
double Pa = 0, Ea = 0;
double e0 = 8.85/1E12;

double get_power_res(double x_, int n_){
      double res = x_;
      for (int i = 0; i < n_ - 1; i++){
```

```
        res = res*x_;
    }
    return res;
}

double func1(){
    int counter = 0, i = 0;
    while (i < n){
        p1[i] = Pa;
        e1[i] = Ea;
        Pa0 = Pa - L*K*(2 * a*Pa + 4 * aa*get_power_res(Pa, 3) + 6 *
aaa*get_power_res(Pa, 5) - Ea + D*Pa/e0);
        Ea += 10;
        Pa = Pa0;
        i++;
    }
    return 0;
}
double fun(){
    func1();
    double Ma = Pa, Na = Ea;
    int counter = 0, j = 0;
    while (j<n) {
        p11[j] = Ma;
        e11[j] = Na;
        Ma0 = Ma - L*K*(2 * a*Ma + 4 * aa*get_power_res(Ma, 3) + 6 *
aaa*get_power_res(Ma, 5) - Na + D*Ma/e0);
        Na -= 10;
        Ma = Ma0;
        j++;
    }
    return 0;
}

int main(){
    fun();
    char fname[100];
    fstream file;
    string delimiter = ",";
```

```
    string filename;
    string filename2;
    string file_dir = "C:\\Users\\sumyuri\\Desktop\\research\\PEFEdata\\";
    stringstream ss;
    stringstream bb;
    ss << T;
    bb << D;
    filename = ss.str();
    filename2 = bb.str();
    string str_file = file_dir + filename +"+"+ filename2 + ".dat";
    sprintf_s(fname, str_file.c_str());
    file.open(fname, ios_base::out);
    file << "TITLE= \"polarization\"" << endl
        << "VARIABLES = \"E\", \"P\"" << endl
        << "ZONE T=\"zone\" DATAPACKING=POINT" << endl
        << endl;
    for (int i = 0; i < n; i++){
        file << e1[i] << delimiter
            << p1[i] << delimiter
            << endl;
    }
    for (int j = 0; j < n; j++){
        file << e11[j] << delimiter
            << p11[j] << delimiter
            << endl;
    }
    file.close();
    return 0;
}
```